# Crystallographic Evidence of a Large Ligand-Induced Hinge–Twist Motion between the Two Domains of the Maltodextrin Binding Protein Involved in Active Transport and Chemotaxis[†,‡]

Andrew J. Sharff,[§] Lynn E. Rodseth,[∥,⊥] John C. Spurlino,[§,#] and Florante A. Quiocho*[,§,∥]

*Howard Hughes Medical Institute and Department of Biochemistry, Baylor College of Medicine, One Baylor Plaza, Houston, Texas 77030*

*Received July 29, 1992; Revised Manuscript Received September 11, 1992*

ABSTRACT: The periplasmic maltodextrin binding protein of *Escherichia coli* serves as an initial receptor for the active transport of and chemotaxis toward maltooligosaccharides. The three-dimensional structure of the binding protein complexed with maltose has been previously reported [Spurlino, J. C., Lu, G.-Y., & Quiocho, F. A. (1991) *J. Biol. Chem. 266*, 5202–5219]. Here we report the structure of the unliganded form of the binding protein refined to 1.8-Å resolution. This structure, combined with that for the liganded form, provides the first crystallographic evidence that a major ligand-induced conformational change occurs in a periplasmic binding protein. The unliganded structure shows a rigid-body "hinge-bending" between the two globular domains by approximately 35°, relative to the maltose-bound structure, opening the sugar binding site groove located between the two domains. In addition, there is an 8° twist of one domain relative to the other domain. The conformational changes observed between this structure and the maltose-bound structure are consistent with current models of maltose/maltodextrin transport and maltose chemotaxis and solidify a mechanism for receptor differentiation between the ligand-free and ligand-bound forms in signal transduction.

D-Maltodextrin binding protein (MBP)[1] is a member of a large group of periplasmic binding proteins of Gram-negative bacteria. Although the entire group is involved as primary components of high-affinity active transport (Furlong, 1987), only a handful (MBP included) serve as initial receptors for bacterial chemotaxis (Macnab, 1987). The three-dimensional structure of MBP ($M_r$ = 40 600) complexed with maltose has been reported to 2.3 Å by Spurlino et al. (1991), although it has now been extended to 1.7 Å (J. C. Spurlino and F. A. Quiocho, unpublished data). The structure shows many similarities with those with specificities for L-arabinose, D-galactose/D-glucose, sulfate, phosphate, leucine/isoleucine/valine, and leucine only (Quiocho & Vyas, 1984; Pflugrath & Quiocho, 1985, 1988; Luecke & Quiocho, 1990; Vyas et al., 1987, 1988, 1991; Sack et al., 1989a,b; Quiocho, 1990), also determined in this laboratory. All of these periplasmic binding proteins are monomeric and have two distinct globular domains, separated by a deep groove or cleft. Each domain has a central $\beta$-pleated sheet, flanked on both sides by two or three parallel $\alpha$-helices. Whereas the structures of ABP, SBP, PBP, and GGBP were determined with bound ligands, those of LIVBP and LBP are free of ligands. The ligands are engulfed in the cleft between the two domains and held in place mainly by hydrogen bond and van der Waals interactions with residues in both domains; these forms are identified as the "closed form". In the structures of the two proteins without bound ligands, the two domains are farther apart and the cleft is wide open (the "open form"). MBP is the first binding protein in which the structures of the closed (liganded) and open (unliganded) forms have been determined and refined at very high resolutions. We have also recently determined and refined at 1.7-Å resolution the structure of the liganded, closed form of LIVBP (S. D. Trakhanov and F. A. Quiocho, manuscript in preparation).

In MBP, the maltodextrin binding site is located at the base of the groove between the two domains (identified as N- and C-domains). As described by Spurlino et al. (1991), bound maltose is almost completely shielded from the bulk solvent and bound by an extensive network of hydrogen bonds and van der Waals interactions, several of which are due to the stacking of aromatic residues against the faces of the pyranose rings. The two domains (N-domain, residues 1–109 and 264–309; C-domain, residues 114–258 and 316–370) are joined by three segments—1 (residues 110–113), 2 (residues 259–263), and 3 (residues 310–315). The first two segments form a short sheet-like structure at the base of the cleft. The third forms a small loop a little further up the side of the cleft and with its apex almost perpendicular to the other two segments.

It has been proposed that membrane-bound receptors recognize and bind to the liganded form of the binding proteins in preference to the unliganded one (Quiocho et al., 1977; Quiocho, 1990), a stringent requirement for the initiation of both active transport and chemotaxis. This model strongly implies that the binding proteins undergo a ligand-induced conformational change, distinguishing the two forms. Indeed, there is strong evidence from a variety of studies using low-angle X-ray scattering (Newcomer et al., 1981), kinetic (Miller

† This work was supported in part by grants from the National Institutes of Health and the Welch Foundation.

‡ Crystallographic coordinates have been deposited in the Brookhaven Protein Data Bank (reference numbers 1OMP, 1OMPSF, and 2MBP).

* To whom correspondence should be addressed.

§ Howard Hughes Medical Institute.

∥ Department of Biochemistry.

⊥ Current address: Howard Hughes Medical Institute, University of Texas Southwestern Medical Center, 5323 Harry Hines Blvd., Dallas, TX 75235.

# Current address: Eastmann-Kodak Co., 1999 Lake Ave., Rochester, NY 14560.

[1] Abbreviations: MBP, maltose/maltodextrin binding protein; ABP, L-arabinose binding protein; GGBP, D-galactose/D-glucose binding protein; SBP, sulfate binding protein; PBP, phosphate binding protein; LIVBP, leucine/isoleucine/valine binding protein; LBP, leucine-specific binding protein; rms, root mean square.

0006-2960/92/0431-10657$03.00/0 

Table I: Molecular Replacement Solution of the Unliganded MBP Structure[a]

| | N-domain | | | C-domain | | |
|---|---|---|---|---|---|---|
| Euler angles (deg)[b] | α (deg) | β (deg) | γ (deg) | α (deg) | β (deg) | γ (deg) |
| Crowther rotation (fine grid) | 335.00 | 97.50 | 155.00 | 310.00 | 115.00 | 125.00 |
| Lattman rotation | 334.50 | 97.75 | 153.50 | 311.75 | 115.75 | 124.75 |

[a] The maltose-bound MBP model contained 2862 atoms and 13 829 reflections between 9- and 5-Å resolution in an artificial 100 × 100 × 100 Å unit cell. The unknown sugar-free MBP contained 1261 reflections in the same resolution range. [b] The Euler angles are defined by Fitzgerald (1988).

et al., 1983; Walmsley et al., 1992), theoretical (Mao et al., 1982), structural (Sack et al., 1989a,b; Quiocho, 1990), site-directed mutagenesis (Vermersch et al., 1990, 1991; Jacobson et al., 1991, 1992), and $^{19}F$ NMR (Luck & Falke, 1991a,b) which indicates that open and closed forms exist and may be interconverted by bending around a hinge between the two domains, a model termed the "Venus flytrap". It is further proposed that the open and closed forms exist in an equilibrium, where ligand binding stabilizes the closed form. This model is similar to that described for a broad range of two-domain proteins which bind substrate in an interdomain cleft (Bennett & Huber, 1984). This proposes that the hinge connecting the domains is flexible while the domains themselves are rigid. Hexokinase and phosphoglycerate kinase are particularly clear examples (Steitz et al., 1976; Graham et al., 1991). More recently, structural studies have shown ligand-induced hinge-bending in apolactoferrin (Anderson et al., 1990).

In addition to MBP, transport across the cytoplasmic membrane requires a membrane-bound heterocomplex of three proteins: MalF (Froshauer & Beckwith, 1984), MalG (Dassa & Hofnung, 1985), and MalK (Gilson et al., 1982). Similarly, chemotaxis involves the Tar (*T*axis to *a*spartate and away from some *r*epellants) signal transducer protein located in the cytoplasmic membrane as a homodimer (Falke & Koshland, 1987). Initiation of both active transport and chemotaxis is presumably achieved by the binding of a ligand-bound MBP molecule to the membrane-bound components.

## EXPERIMENTAL PROCEDURES

MBP was isolated and purified according to a previously described protocol (Spurlino et al., 1991). Crystals suitable for high-resolution data collection were obtained using the hanging-drop method. Drops (13% PEG 20K, ≈6 mg/mL MBP, 20 mM MES, pH 6.2) were suspended over 30% PEG 20K in Linbro tissue culture plates at room temperature (≈21 °C). Small crystals usually appeared within a few weeks. These were used for macroseeding in 21% PEG drops placed over 25% PEG and grew to usable size within 3–4 weeks.

Intensity data were collected from a single crystal to 1.73 Å on an ADSC two-area detector system mounted on a Rigaku RU-200 rotating anode (Cu Kα 1.5418 Å) with a graphite monochromator and operated at 100 kV and 40 mA. The data were collected according to the protocol described by Xuong et al. (1985). Data reduction and scaling were carried out using the Howard et al. (1985) software package, implemented by Nielsen for the ADSC.

The structure was determined by molecular replacement using the MERLOT package (Fitzgerald, 1988) with the maltose-bound MBP structure refined at 1.7-Å resolution as the search model. Model fitting to electron density and visual analysis were performed using the program CHAIN (Sack, 1988). Refinement of the fitted structure was carried out using the program packages XPLOR (Brünger, 1990) and PROLSQ (Hendrickson & Konnert, 1980).

## RESULTS

*Crystallization and Diffraction Data.* Crystals of the unliganded form of MBP are triclinic, unlike the monoclinic crystals of the maltose-loaded MBP (Spurlino et al., 1991). Typically, their dimensions are in the order of 0.6 × 0.6 × 0.4 mm. Analysis of precession photographs and diffraction data obtained from the area detector identified their space group as $P1$, with cell dimensions $a$ = 38.35 Å, $b$ = 44.44 Å, $c$ = 58.25 Å, $\alpha$ = 101.0°, $\beta$ = 100.4°, and $\gamma$ = 104.2°, with one molecule of 40 600 Da in the unit cell. The calculated volume and dimensions of this cell are barely larger than those of the MBP molecule, indicating close crystal packing is likely. A total of 107 789 observations of 33 722 unique reflections were collected to 1.73 Å (91% complete) with a merging $R$-value of 5.67 (on $I$) and $\langle F/\sigma F\rangle$ = 20. However, due to the completeness of the shell outside 1.8 Å and strength of the data, only 2$\sigma$ data between 10.0 and 1.8 Å were used for structure refinement, a total of 28 238 unique reflections.

*Molecular Replacement.* Structure determination by molecular replacement was carried out in two stages. In all cases, rotation functions were calculated with $F_o$ between 9- and 5-Å resolution with a Patterson cutoff radius of 25 Å (Crowther rotation only). Initially, the whole maltose-bound MBP structure (excluding water molecules) was used as the search model in the cross rotation, but although this gave a clear solution ($\alpha$ = 320.0°, $\beta$ = 105.0°, $\gamma$ = 135.0°), all subsequent attempts at structure refinement were unsuccessful. The structure would not refine to an $R$-value below 43%, and electron density maps were uninterpretable. Subsequently, the MBP molecule was split through the center of the three interdomain segments (at residues 111, 261, and 312), into its N- and C-domains. Cross-rotation functions were then recalculated using each domain separately as the search model. Both cases gave very strong solutions (peaks over 10$\sigma$ and at least 3 times bigger than the next highest peak), with Eulerian angles differing by ≈20° in $\alpha$, $\beta$, and $\gamma$ (see Table I). These solutions were then applied to the respective domains, and the $x$, $y$, and $z$ translations of the rotated N-domain were visually manipulated relative to the rotated C-domain using CHAIN to "reanneal" the cut hinge segments as closely as possible. Using this "rebuilt" structure in the cross-rotation function gave a 12$\sigma$ peak at $\alpha$ = 0°, $\beta$ = 0°, and $\gamma$ = 0°, with an absolute height an order of magnitude larger than that using the individual domains. The initial $R$-value, calculated with this model, was 45%.

*Refinement.* An initial rigid-body refinement, carried out using XPLOR and allowing the two domains to move relative to each other, reduced the $R$-value to 35%. Subsequent molecular dynamics refinement further reduced the $R$-value to 26%. Several cycles of manipulation of the structure in the density of the 1.8-Å maps, calculated with $(2|F_o| - |F_c|, \alpha_c)$ and $(|F_o| - |F_c|, \alpha_c)$, building in 77 well-defined water molecules, followed by conventional positional and $B$-factor refinement using XPLOR were performed. After a final cycle with PROLSQ the refinement converged with an $R$-value of 21%. Table II gives a summary of the refinement parameters.

The geometry of the refined sugar-free structure is very good (Table II), with only three residues violating the Ramachandran plot. Furthermore, Luzatti plot analysis shows that the expected error in the coordinates is low, around 0.20

Table II: Refinement and Geometry Statistics for Unliganded MBP[a]

| | |
|---|---|
| resolution range | 10.0–1.8 Å |
| no. of reflections (with $2\sigma$ cutoff) | 28 238 |
| completeness | 86% |
| $R$-value | 0.210 |
| protein atoms | 2862 |
| ordered waters | 77 |
| bond distances | 0.015 Å (0.020 Å) |
| angle distances | 0.031 Å (0.030 Å) |
| dihedral distances | 0.040 Å (0.050 Å) |
| planar group distances | 0.013 Å (0.020 Å) |
| peptide $\omega$ angle | 2.200° (3.000°) |
| chiral volume | 0.178 Å$^3$ (0.150 Å$^3$) |

[a] Numbers in parentheses represent the stereochemical restraints applied by PROLSQ.

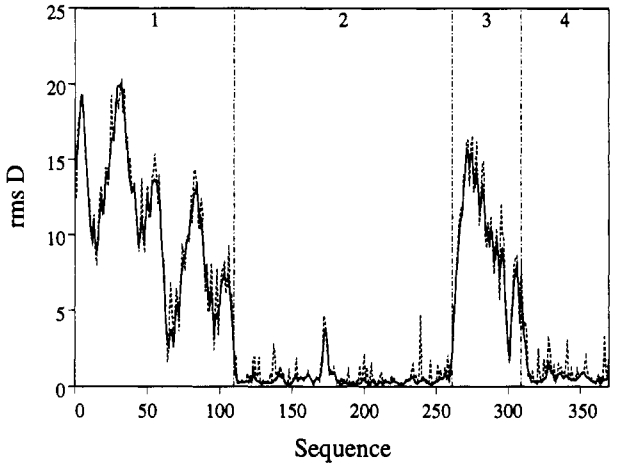


FIGURE 1: Plot of rms deviation in coordinates (in Å) of the overlapped structures of the unliganded and maltose-bound forms of MBP, calculated by XPLOR. Superposition was performed by the program SHP, written by D. I. Stuart [using the method of Rossmann and Argos (1977)]. Deviations in the $C_\alpha$ backbones are shown as a solid line and deviations in side chains as a broken line. The four sections of the polypeptide chain are marked: 1 (residues 1–110), 2 (residues 111–261), 3 (residues 262–309), and 4 (residues 310–370).

Å across the entire resolution range. The individual domains from both the maltose-bound and sugar-free structures were superimposed for separate analysis. The superimposed C-domains show more rms deviation (0.72 Å) than the smaller N-domains (0.37 Å); however, in both cases, deviations of the $\alpha$-carbon backbone were within acceptable limits. The observed small deviations are randomly distributed throughout the whole structure. The only significant deviation in the backbone is seen in the C-domain, involving residues 172–174 (Glu-Asn-Gly). These residues have no involvement in ligand binding. Furthermore, the overall rms deviations for the side chains for either domain were less than 2 Å. Analysis of the whole structures was performed by superimposition of the C-domains (as the larger of the two); see Figure 1. This graphically illustrates the rigid-body nature of the change between the ligand-free and ligand-bound forms.

## DISCUSSION

The quality of the electron density maps was very high with little or no significant density, either positive or negative, in ($|F_o|-|F_c|$, $\alpha_c$) maps, even contouring as low as $0.8\sigma$. The final $R$-value is rather high when compared to the maltose-bound structure (16.4% to 1.7 Å) or other structures of binding proteins refined to comparable resolution in this laboratory (e.g., ABP, GGBP, PBP, and SBP). Nevertheless, all the indications from geometric analysis, as well as visual inspection of both the electron density and model, show that the structure has been well refined.

Table III: $\phi$ and $\psi$ Angles (deg) of the Three Hinge Residues in the Unliganded (Open Form) and Maltose-Bound (Closed Form) Structures

| | unliganded | | liganded | |
|---|---|---|---|---|
| residue | $\phi$ | $\psi$ | $\phi$ | $\psi$ |
| Glu 111 | −136 | 138 | −105 | 130 |
| Val 261 | −125 | 116 | −108 | 103 |
| Ala 312 | −63 | −2 | −162 | 103 |

The overall isotropic $B$-factor is low at 22.1 Å$^2$ and agrees well with the $B$-factor given from a Wilson plot (19.4 Å$^2$). This is lower than that for the maltose-bound structure refined to 1.7 Å (30.8 Å$^2$), which is somewhat surprising. The pattern of individual $B$-factors, both backbone and side chain, is similar in both structures, the external loops and helices having the highest values. Residues making both polar and apolar interactions with the maltose are all situated at minima as would be expected. The $B$-factors for those residues making direct or water-mediated hydrogen bonds to maltose are 25% higher in the unliganded structure; however, the $B$-factors for polar or indeed all residues in the binding cleft are only 5% higher in the unliganded form.

Relatively few ordered water molecules were found (Table II), compared to the maltose-loaded structure (142 waters), many of which are located in or around the sugar binding cleft. Closer analysis shows a number of unexpected features. It is noteworthy that far fewer ordered water molecules were found in the wide-open cleft in the unliganded structure (21) than in the maltose-bound structure (35), eight of which are wholly or partially conserved (making similar interactions with the protein in both structures). Of these, only one is involved in maltose binding, accepting a hydrogen bond from the side-chain hydroxyl of Tyr 155 and donating a hydrogen bond to the C3 hydroxyl of the reducing sugar of the maltose. Contrary to expectation, many of the polar groups that are involved in hydrogen bonding the bound maltose (Spurlino et al., 1991) lack bound, ordered water molecules. Nevertheless, a large volume of the binding cleft is almost certainly filled with disordered water.

Of particular interest is that this structure, taken together with the maltose-bound structure, shows that MBP exhibits a near classic hinge-bending in response to sugar binding. The individual domains are barely changed between the two forms; perturbations of mostly the aromatic residues lining the binding cleft are of note. These include those making hydrophobic stacking interactions with the bound sugar (i.e., Trp 62, Tyr 155, Trp 230, and Trp 340), which have become somewhat more flattened against the sides of the binding cleft, presumably to minimize their exposure to the solvent. Increased interaction between these side chains and the core framework reduces their flexibility, accounting for their $B$-factors, averaging 15% lower than those observed in the maltose-bound structure. There is little change in the orientation of the polar residues in the cleft, with the exception of Glu 111.

The main structural changes observed are mediated entirely by bending of the main chain of the hinge segments (Table III). The major motion is the hinge opening about an axis through the center (residues 111 and 261) of hinge segments 1 and 2 (see Figure 2a). This motion is due to roughly equivalent changes in both $\phi$ and $\psi$ angles of single residues (Glu 111, $\Delta\phi = 31°$ and $\Delta\psi = -8°$; Val 261, $\Delta\phi = 17°$ and $\Delta\psi = -13°$). The observed increase in the hinge angle as a result of this motion has been measured at 35° (Figure 2b).

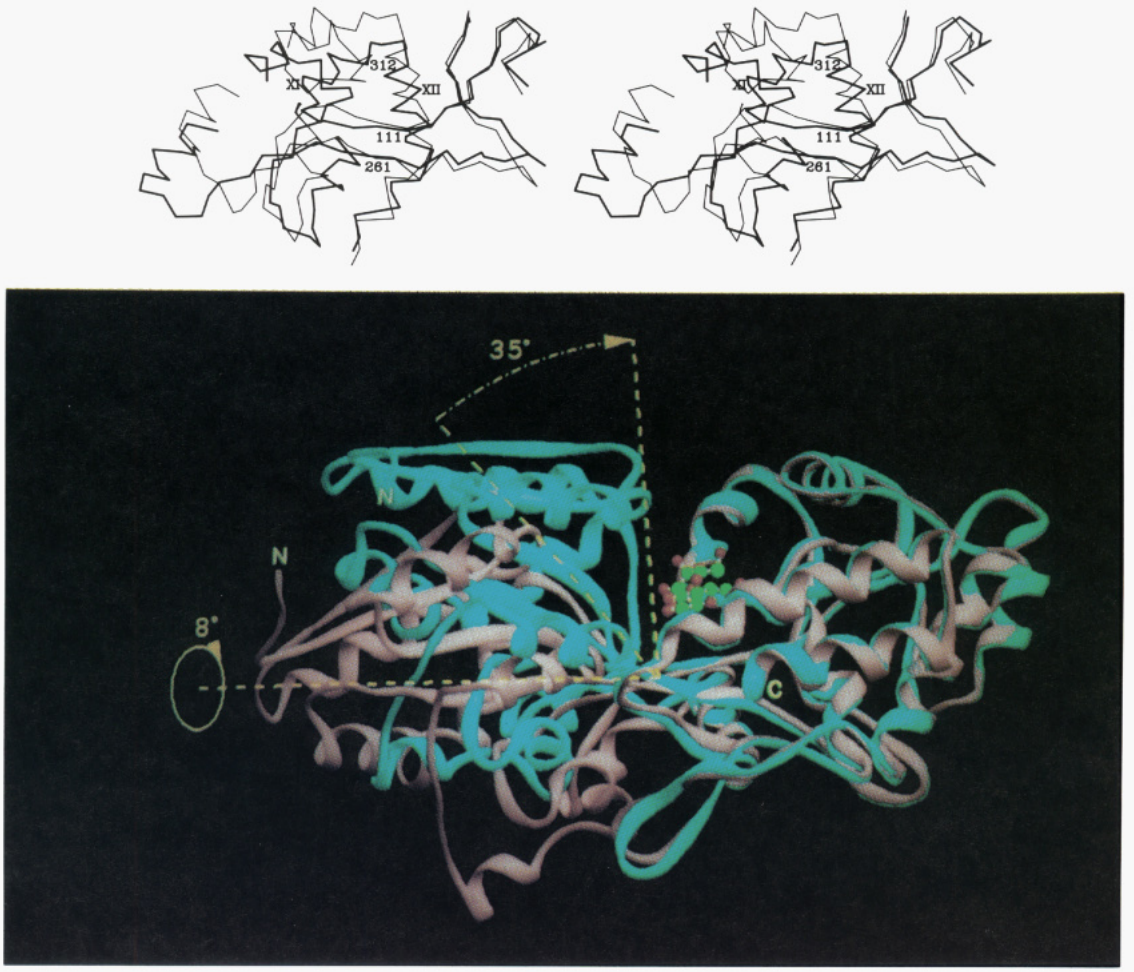


FIGURE 2: (a, top) Stereoview of the superimposed backbone structure on the hinge region of the open, unliganded (thick line) and closed, maltose-bound (thin line) structures of MBP, looking down into the binding cleft. The central hinge residues and helices XI and XII are indicated. (b, bottom) Perspective view of the superimposed backbone structures of unliganded (mauve) and maltose-bound (blue) MBP (looking into the binding cleft from the side) with bound maltose (ball and stick model). The direction and magnitude of the conformational change going from the unliganded to ligand-bound form are shown. The picture was obtained using the RIBBONS program of M. Carson (1987).

Compared to other periplasmic binding proteins, the opening angle in MBP is roughly comparable with that deduced (30°) in comparing the unliganded (open form) structure of LIVBP with the liganded (closed form) structure of ABP (Sack et al., 1989a) but nearly twice the opening angle of 18° deduced in $^{19}F$ NMR studies of GGBP (Luck & Falke, 1991a).

A new finding, which is most unusual, is the effect of the third hinge segment in the interdomain rotation of MBP. This segment links a helix (XI) of the N-domain to a helix (XII) of the C-domain. Both helices XI and XII are packed closely against the $\beta$-sheets of their respectively domains (Spurlino et al., 1991). The strength of the packing interactions between the helices and the domain sheets constrains the flexibility and geometrical rearrangement of the hinge. This results in the N-domain being pulled over toward interdomain segment 3 as the hinge opens, deforming this segment (Figure 2a), and is seen as an 8° anticlockwise rotation of the N-domain relative to the C-domain (Looking down an axis through the N-domain toward the C-domain) (Figure 2b). The "strain" on the central residue (Ala 312) between the two helices in segment 3 is evident by the large shifts (in its $\phi$ and $\psi$ angles) (Table III) in going from the open form to the closed form (–99° and 101°, respectively). It is noteworthy that these torsion angle changes are radically different from the similar changes observed for Glu 111 and Val 261 in segments 1 and 2, respectively (Table III).

MBP is similar to the other binding proteins and many other single polypeptide, two-domain proteins, such as hexokinase and phosphofructokinase, in that the hinge is composed of two or three segments. Very few proteins, such as lysozyme, have a single segment domain linkage. The advantage of a single-stranded hinge is a wide degree of flexibility, allowing the two domains considerable conformational freedom. However, for many large proteins too much flexibility may be a considerable disadvantage. The addition of a second or third connecting segment reduces the flexibility of the hinge and restricts the possible modes of domain movement in a manner similar to that seen in the MBP system.

On the basis of the pattern and number of sugar–protein interactions observed in the maltose-bound MBP structure, Spurlino et al. (1991) proposed that maltose binds first to one domain (probably the N-domain) in the open form. A similar proposal was originally advanced by Sack et al. (1989a) as a result of the crystallographic studies of the LIVBP and in analyzing the interactions between ligands and the two domains of ABP, GGBP, and SBP. Of the polar residues involved in binding maltose to MBP, Glu 111 is significant in the ligand-induced hinge–twist interdomain motion in that it is located at the base of the binding cleft, in the middle of hinge segment 1, with the side-chain carboxylate OE2 accepting a hydrogen bond from the C2 hydroxyl of the reducing glucosyl unit of maltose. In going from the open cleft, unliganded structure

FIGURE 3: Stereoview of the superimposed backbone of hinge segment 1 highlighting the side chain of Glu 111 and its interaction (dashed line) with bound maltose: unliganded (thin line); maltose bound (thick line).

FIGURE 4: Stereo space-filling representation of both maltose-bound (a, top) and unliganded (b, bottom) MBP, looking down into the binding cleft. The N-domain is shown in blue, the C-domain in yellow, and maltose in red. Positions of mutations affecting maltodextrin transport are shown in white and mutations affecting chemotaxis in green.

to the closed, maltose-loaded structure, there is a concerted (≈4 Å) shift of the Glu 111 side chain, moving up into the cleft as a result of sugar binding (Figure 3). This ligand-induced movement of Glu 111 may be the triggering mechanism for the motion that enables the other domain to participate in ligand binding and to ultimately engulf the bound oligosaccharide.

The results described here, combined with those obtained from the structure determination of MBP complexed with maltose, provide the first crystallographic proof that a periplasmic receptor for both active transport and chemotaxis exists in an open form which is converted, by way of hinge-bending and twisting motion between the two domains, to a closed form on ligand binding. Similar evidence has been obtained recently from the structure analysis of LIVBP complexed with leucine (S. D. Trakhanov and F. A. Quiocho, unpublished data). The determination of the first X-ray structure of a periplasmic binding protein presaged the existence of these two forms and in part the motion that interconverts the two (Quiocho et al., 1977).

In the course of our high-resolution structure analysis of seven binding proteins, we have thus far determined the structures of all four possible structural forms—the open unliganded form, the open liganded form, the closed liganded form, and the closed unliganded form (Quiocho, 1990). The open unliganded form is typified by MBP (structure described herein), LIVBP (Sack et al., 1989a), and LBP (Sack et al., 1989b). We have also determined the structure of a "super-open" form of LIVBP in which the hinge-bending angles between the two domains are larger and the cleft is more open than in the structure of the unliganded form first determined for LIVBP (Sack et al., 1989a; S. D. Trakhanov, H. Luecke,

and F. A. Quiocho, unpublished data). The binding of leucine exclusively to one domain of the open unliganded form of LIVBP is an example of the open liganded form (Sack et al., 1989a). Examples of the closed liganded form are more abundant; they include the structures of MBP (Spurlino et al., 1991), ABP (Quiocho & Vyas, 1984; Vyas et al., 1991), GGBP (Vyas et al., 1987, 1988, 1991), SBP (Pflugrath & Quiocho, 1985, 1988), PBP (Luecke & Quiocho, 1990), and LIVBP (S. D. Trakhanov and F. A. Quiocho, unpublished data). We have also determined the structure of ABP without bound sugar that is similar to the structure of the closed liganded form (N. K. Vyas, M. N. Vyas, and F. A. Quiocho, unpublished data). Although many proteins have been shown or implicated to undergo ligand-induced hinge-bending motion (Bennett & Huber, 1984), to our knowledge only the structural analysis of the periplasmic binding proteins has revealed the existence of all four possible stable forms. Other laboratories have also determined the structures of the closed liganded form of GGBP (Mowbray et al., 1990) and ribose binding protein (Mowbray & Cole, 1992) and the closed unliganded form of the lysine/arginine/ornithine binding protein (Kang et al., 1991).

MBP exists in a dynamic equilibrium between the open and closed forms. The major force driving hinge closing MBP is probably the exclusion of water from the binding site, maximizing interdomain salt link, electrostatic and hydrophobic interactions. It is possible that the open form is favored in the absence of ligand as the solvent trapped in the ligand binding site would make it energetically unfavorable to close. Sugar binding, however, maximizes solvent exclusion (entropic effect) and pushes the equilibrium over to favor the closed form. As the two domains participate in sugar binding, the closed liganded form is also stabilized. The shift in the equilibrium on sugar binding may also be encouraged by the interaction of the sugar with Glu 111—the resulting perturbation of the hinge favoring the closed form.

The degree of opening of the hinge is much greater than one might expect if the sole function was to allow free access of maltooligosaccharides to the binding site. Indeed, the increase in accessibility of the binding site in the open form (the solvent-accessible area increases by 170 Å$^2$) would allow unrestricted entry to maltodextrins much larger than MBP will actually bind. A more powerful explanation for such a large conformational change is based on the effect on signal transduction in both active transport and chemotaxis (Jacobson et al., 1992). The membrane-bound receptors, distinct for each process, must have a unique preference to bind to the liganded form of MBP. Otherwise, no differentiation between the presence or absence of ligand would be possible, an effect deleterious to both active transport and chemotaxis.

A large number of MBP mutants have been isolated with varying effects on either maltodextrin binding and transport or chemotaxis or both (Duplay et al., 1987; Duplay & Szmelcman, 1987; Treptow & Shuman, 1985, 1988; Kossmann et al., 1988; Martineau et al., 1990; Zhang et al., 1992). The sites of these mutations as mapped on the structure are clustered on a single face of the protein surface, at the top end of the N- and C-domains at the same side as the opening of the cleft (Spurlino et al., 1991). Many of the mutations affecting transport or chemotaxis are spatially distinct and are distributed quite differently. The locations of some of the more critical mutations in MBP are portrayed in Figure 4.

This face of the MBP molecule, in the closed form, constitutes the recognition/binding site for the receptors for both transport and chemotaxis. This is supported by the identification of countermutations in the Tar receptor which restore some chemotactic activity in two of the chemotactic-deficient MBP mutants (Kossmann et al., 1988). The structure of the open form illustrates graphically a mechanism by which both transport and chemotaxis systems may differentiate between ligand-free and ligand-bound MBP (Quiocho, 1990). It is clear that, in the ligand-free form, the opening of the two domains completely destroys the ensemble of the receptor binding site. The overall motion is such that residues at opposite ends of the face have moved by up to 20 Å. The twisting of the N-domain disrupts the binding site more than simple hinge opening alone, further ensuring that the open form cannot make a productive interaction with the membrane-bound components of each process.

The nature of the interaction of MBP with Tar is unclear as to whether MBP interacts with one or both of the subunits of the homodimer. Recent work suggests that it is unlikely that MBP interacts with a single subunit (Zhang et al., 1992). However, the structure of the ligand binding domain of the *Salmonella typhimurium* Tar receptor, which is highly homologous to the *Escherichia coli* Tar receptor, has recently been reported (Milburn et al., 1991). Comparison of these two should enable further study into the exact nature of its interaction with MBP.

The equilibrium position of open/closed MBP is shifted to heavily favor the open form in the absence of ligands, to minimize the interaction between the receptors and ligand-free MBP molecules in the closed form. Sugar binding shifts the equilibrium over the other way, by the participation of the two domains in binding and possibly by the effect of the hydrogen bond interaction of the sugar with Glu 111 in the hinge. The large structural change in going from the unliganded to the liganded form of MBP is best described as a combination of hinge-bending and twisting motions between the two domains. This description may be more suitable for other proteins that undergo ligand-induced domain motions.

## ACKNOWLEDGMENT

We thank Bill Meador for setting up and collecting the intensity data. We also thank Drs. N. K. Vyas and R. Chattopadhyaya for helpful discussions and assistance.

## REFERENCES

Anderson, B. F., Baker, H. M., Norris, G. E., Rumball, S. V., & Baker, E. N. (1990) *Nature (London) 344*, 784–787.

Bennett, W. S., & Huber, R. (1984) *Crit. Rev. Biochem. 15*, 291–384.

Brünger, A. T. (1990) *X-PLOR, Version 2.1*, Yale University, New Haven, CT.

Carson, M. C. (1987) *J. Mol. Graphics 5*, 103.

Dassa, E., & Hofnung, M. (1985) *EMBO J. 4*, 2287–2293.

Duplay, P., & Szmelcman, S. (1987) *J. Mol. Biol. 194*, 675–678.

Duplay, P., Szmelcman, S., Bedouelle, H., & Hofnung, M. (1987) *J. Mol. Biol. 194*, 663–673.

Falke, J. J., & Koshland, D. E., Jr. (1987) *Science 237*, 1596–1600.

Fitzgerald, P. M. D. (1988) *J. Appl. Crystallogr. 21*, 273–278.

Froshauer, S., & Beckwith, J. (1984) *J. Biol. Chem. 259*, 10896–10903.

Furlong, C. E. (1987) in *Escherischia Coli and Salmonella typhimurium: Cellular and Molecular Biology* (Neidhardt, F. C., Ingraham, J. L., Low, K. B., Magasanik, B., Schaechter, M., & Umbarger, H. E., Eds) pp 786–796, American Society for Microbiology, Washington, DC.

Gilson, E., Higgins, C. F., Hofnung, M., Ames, G. F.-L., & Nikaido, H. (1982) *J. Biol. Chem. 257*, 9915–9918.

Graham, H. C., Williams, R. J., Littlechild, J. A., & Watson, H. C. (1991) *Eur. J. Biochem. 196*, 261–269.
Hendrickson, W. A., & Konnert, J. H. (1980) in *Computing in Crystallography*, pp 13.01–13.23, Indian Academy of Science, Bangalore.
Howard, A. J., Neilsen, C., & Xuong, N. H. (1985) *Methods Enzymol. 114*, 452–472.
Jacobson, B. L., He, J. J., Vermersch, P. S., Lemon, D. D., & Quiocho, F. A. (1991) *J. Biol. Chem. 266*, 5220–5225.
Jacobson, B. L., He, J. J., Lemon, D. D., & Quiocho, F. A. (1992) *J. Mol. Biol. 223*, 27–30.
Kang, C.-H., Shin, W.-C., Yamagata, Y., Gokeen, S., Ames, G. F., & Kim, S.-H. (1991) *J. Biol. Chem. 266*, 23893–23899.
Kossmann, M., Wolff, C., & Mason, M. D. (1988) *J. Bacteriol. 170*, 4516–4521.
Luck, L. A., & Falke, J. J. (1991a) *Biochemistry 30*, 4248–4256.
Luck, L. A., & Falke, J. J. (1991b) *Biochemistry 30*, 4257–4261.
Luecke, H., & Quiocho, F. A. (1990) *Nature (London) 347*, 402–406.
Macnab, R. (1987) in *Escherischia coli and Salmonella typhimurium: Cellular and Molecular Biology* (Neidhardt, F. C., Ingraham, J. L., Low, K. B., Magasanik, B., Schaechter, M., & Umbarger, H. E., Eds.) pp 732–759, American Society for Microbiology, Washington, DC.
Mao, B., Pear, M. R., McCammon, J. A., & Quiocho, F. A. (1982) *J. Biol. Chem. 257*, 1131–1133.
Martineau, P., Saurin, W., Hofnung, M., Spurlino, J. C., & Quiocho, F. A. (1990) *Biochimie 72*, 397–402.
Milburn, M. W., Privé, G. G., Milligan, D. L., Scott, W. G., Yeh, J., Jancarik, J., Koshland, D. E., Jr., & Kim, S.-H. (1991) *Science 254*, 1342–1347.
Miller, D. M. I., Olson, J. S., Pflugrath, J. W., & Quiocho, F. A. (1983) *J. Biol. Chem. 258*, 13665–13672.
Mowbray, S. L., & Cole, L. B. (1992) *J. Mol. Biol. 225*, 155–175.
Mowbray, S. L., Smith, R. D., & Cole, L. B. (1990) *Receptor 1*, 41–45.
Newcomer, M. E., Lewis, B. A., & Quiocho, F. A. (1981) *J. Biol. Chem. 256*, 13218–13222.
Pflugrath, J. W., & Quiocho, F. A. (1985) *Nature (London) 314*, 257–260.
Pflugrath, J. W., & Quiocho, F. A. (1988) *J. Mol. Biol. 200*, 163–180.
Quiocho, F. A. (1990) *Philos. Trans. R. Soc. London 326*, 341–351.
Quiocho, F. A., & Vyas, N. K. (1984) *Nature (London) 310*, 381–386.
Quiocho, F. A., Gilliland, G. L., & Phillips, G. N., Jr. (1977) *J. Biol. Chem. 252*, 5142–5149.
Rossmann, M. G., & Argos, P. (1977) *J. Mol. Biol. 109*, 99–129.
Sack, J. S. (1988) *J. Mol. Graphics 6*, 244–245.
Sack, J. S., Saper, M. A., & Quiocho, F. A. (1989a) *J. Mol. Biol. 206*, 171–191.
Sack, J. S., Trakhanov, S. D., Tsigannik, I. H., & Quiocho, F. A. (1989b) *J. Mol. Biol. 206*, 193–207.
Spurlino, J. C., Lu, G.-Y., & Quiocho, F. A. (1991) *J. Biol. Chem. 266*, 5202–5219.
Steitz, T. A., Fletterick, R. J., Anderson, W. F., & Anderson, C. M. (1976) *J. Mol. Biol. 104*, 197.
Treptow, N. A., & Shuman, H. A. (1985) *J. Bacteriol. 163*, 654–660.
Treptow, N. A., & Shuman, H. A. (1988) *J. Mol. Biol. 202*, 809–822.
Vermersch, P. S., Tesmer, J. J., Lemon, D. L., & Quiocho, F. A. (1990) *J. Biol. Chem. 265*, 16592–16603.
Vermersch, P. S., Lemon, D. D., Tesmer, J. J., & Quiocho, F. A. (1991) *Biochemistry 30*, 6861–6866.
Vyas, N. K., Vyas, M. N., & Quiocho, F. A. (1987) *Nature (London) 327*, 635–638.
Vyas, N. K., Vyas, M. N., & Quiocho, F. A. (1988) *Science 242*, 1290–1295.
Vyas, N. K., Vyas, M. N., & Quiocho, F. A. (1991) *J. Biol. Chem. 266*, 5226–5237.
Walmsley, A. R., Shaw, J. G., & Kelly, D. J. (1992) *J. Biol. Chem. 267*, 8064–8072.
Xuong, N. H., Nielsen, C., Hamlin, R., & Anderson, D. (1985) *J. Appl. Crystallogr. 18*, 342–350.
Zhang, Y., Conway, C., Rosato, M., Suh, Y., & Manson, M. D. (1992) *J. Biol. Chem.* (in press).